Complexity Project: The Oslo Model

Kei Tsun Yeung

19-2-2018

Abstract: The Oslo model as a demonstration of self-organised criticality was studied, with particular respect to the height and avalanche size of the pile. By deriving scaling relationships, determining their parameters and performing data collapse on the height, height probability and avalanche size probability, the scale-free behaviour of such a system was observed. These were found to follow a power law and had a cutoff due to the finite size of the system. However, corrections to scaling were found to be significant with small system sizes for the cross-over time, average height and its standard deviation, and also the second and above moments of avalanche-size probability.

Word count: 2459 in report

1 Introduction

Self-organised criticality refers to a situation in which the response of a system's observables to a slowly-driven perturbation is independent of its scale. The Bak-Tang-Wiesenfeld (BTW) model [1] is the first to demonstrate such behaviour through the continuous addition of grains into a pile. The response is an avalanche which dissipates potential energy stored in the pile once the gravitational force along the slope exceeds the friction. This can be simulated by defining a *constant* threshold slope between each position (site) and the next, such that an avalanche is triggered whenever this is surpassed by the local slope. The Oslo model [2] [3] generalises this by randomising the threshold slope at each site to simulate the difference in orientation of the grains.

2 The Oslo model

2.1 Theory and Algorithm

The 1D system consists of L sites $i = 1, 2, ..., L$, each with a height h_i which measures the number of grains contained [4]. The local slope at site i is defined as $z_i = h_i - h_{i+1}$ between the current site and the next, with $h_{L+1} = 0$. Each site i is assigned a random threshold slope z_i^{th} of either 1 or 2. The system is driven by increasing the height h_1 and slope z_1 by 1 to simulate the addition of a grain. Relaxation (toppling to the next site) is triggered when $z_i > z_i^{th}$, and is achieved for different sites as shown in equation 3. A new z_i^{th} is selected for each relaxed site. The detailed algorithm is as given below.

1. *Initialisation*: Set h_i and z_i to zero and choose random initial threshold slope $z_i^{th} \in \{1, 2\}$ for all i using `numpy.random.choice` with a probability distribution of

$$z_i^{th} = \begin{cases} 1 & \text{with probability} \quad p \\ 2 & \text{with probability} \quad 1 - p \end{cases} \tag{1}$$

   with $p = 1/2$ for this project.

2. *Drive*: Add a grain at site $i = 1$ by

$$z_1 \to z_1 + 1, \quad h_1 \to h_1 + 1. \tag{2}$$

3. *Relaxation*: If $z_i > z_i^{th}$, relax site i.
   For $i = 1$:

$$\begin{aligned} z_1 &\to z_1 - 2, \quad h_1 \to h_1 - 1, \\ z_2 &\to z_2 + 1, \quad h_2 \to h_2 + 1. \end{aligned} \tag{3a}$$

   For $i = 2, ..., L - 1$:

$$\begin{aligned} z_i &\to z_i - 2, \quad h_i \to h_i - 1, \\ z_{i\pm1} &\to z_{i\pm1} + 1, \quad h_{i+1} \to h_{i+1} + 1. \end{aligned} \tag{3b}$$

For $i = L$:

$$z_L \rightarrow z_l - 1, \quad h_L \rightarrow h_L - 1,$$
$$z_{L-1} \rightarrow z_{L-1} + 1. \tag{3c}$$

Choose a new threshold slope at random for each relaxed site $z_i^{th} \in \{1, 2\}$ using equation 1. The previous site $i - 1$ is then revisited to determine whether further avalanches are needed until all sites have been properly relaxed.

4. *Iteration*: Return to step **2**.

2.2 Implementation and Test - Task 1

To test if the program was working properly, the average slope $\langle z \rangle$ of all sites was plotted against the number of grains added (defined as time t) for probabilities $p = 0.0$, 0.5, 1.0 in Figures 1a, 2 and 1b respectively for system sizes $L = 4, 8, 16, 32, 64, 128, 256$. It is worth noting that $p = 0.0$ and 1.0 correspond to the BTW model while $p = 0.5$ corresponds to the Oslo model.
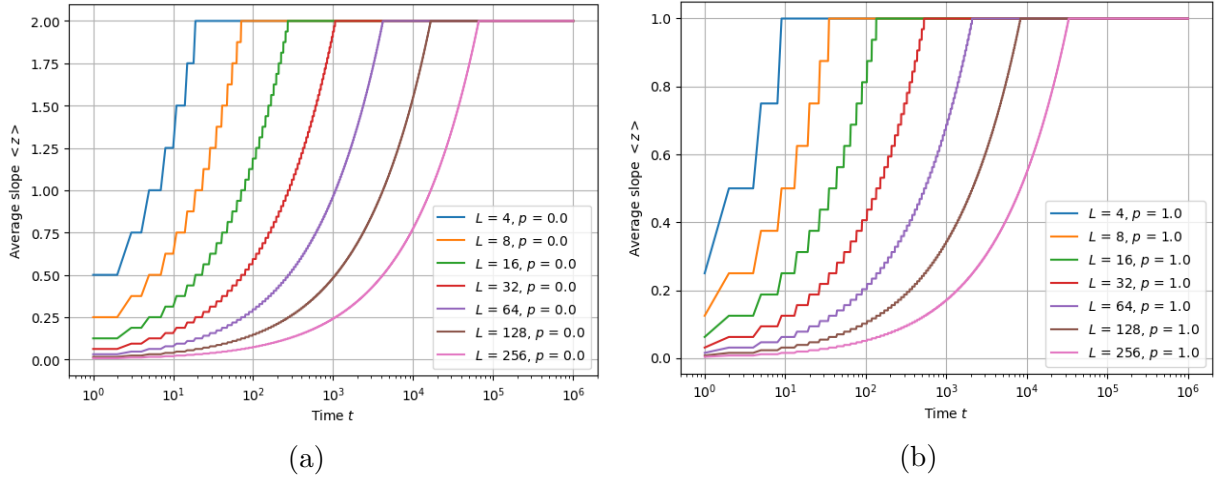

(a)   (b)

Figure 1: Graphs of average slope $\langle z \rangle$ against number of grains added (time) t for $p =$ (a) 0.0 and (b) 1.0 for system sizes L ranging from 4 to 256. The average slope tended towards 2 and 1 respectively as expected, equal to the chosen threshold slopes.

Since the threshold slope was constant across all sites for $p = 0.0$ and 1.0, as the system reached equilibrium, all the local slopes were expected to tend towards the chosen slope and this can be confirmed in Figure 1.

Following the same argument, $p = 0.5$ should yield a steady-state average slope of 1.5, but this is not the case in Figure 2, around 1.73. Also, it fluctuates greatly for small system size but decreases in amplitude as L became large. The average slope was greater than expected because a threshold slope z^{th} of 2 was more stable and triggered less avalanches than 1 when grains were added, so the system had an average slope closer to 2. The fluctuations become smaller since there were a larger number of sites to average the slopes over.
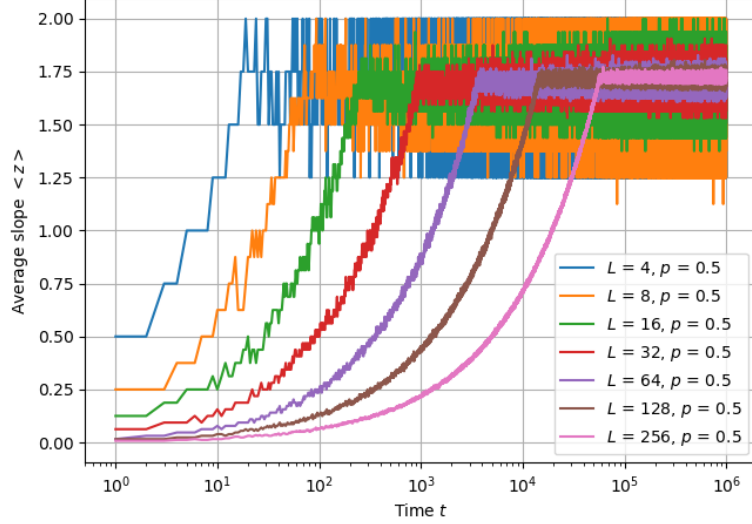
Figure 2: Graph of average slope $\langle z \rangle$ against number of grains added (time) t for $p = 0.5$ for system sizes L ranging from 4 to 256.

3 Height of the pile $h(t; L)$ and cross-over time $t_c(L)$

From this task onwards (except Task 2d), data were taken for system sizes $L = 2$, 4, 8, 16, 32, 64, 128, 256, 512, 1024 and total number of grains added $= 10^7$.

3.1 Height of the pile $h(t; L)$ - Task 2a

The height of the pile $h(t; L)$ is defined as the height at site 1 h_1 after the pile reaches a stable configuration with each added grain [4]. Figure 3 show how the height evolved with each added grain.

Two configurations can be identified: transient and recurrent. During the transient, the height increased according to a power law of t, as shown by the linear increase in log-log scale in Figure 3b. Recurrence was reached when the height fluctuated around a stable average. The height no longer increased after recurrence because all the local slopes were matching the threshold slopes and any added grain simply dropped out of the system. The fluctuations are due to the fact that the threshold slopes were changing whenever an avalanche occurs.

3.2 Scaling relation and data collapse - Tasks 2b and c

When system size $L \gg 1$ and in steady state, the local slopes can be approximated to be smoothed out to be the average slope $\langle z \rangle$ as shown in Figure 4. In this case, the height can be obtained as $\langle z \rangle L \propto L$.

The cross-over time $t_c(L)$ is defined as the number of grains added before an added grain induces a grain to first leave the system [4], and is a measure of reaching recurrence. Since each grain has an area of unity, the number of grains in the pile can be approximated as the area of the triangle in Figure 4 $= \langle z \rangle L^2/2 \propto L^2$.
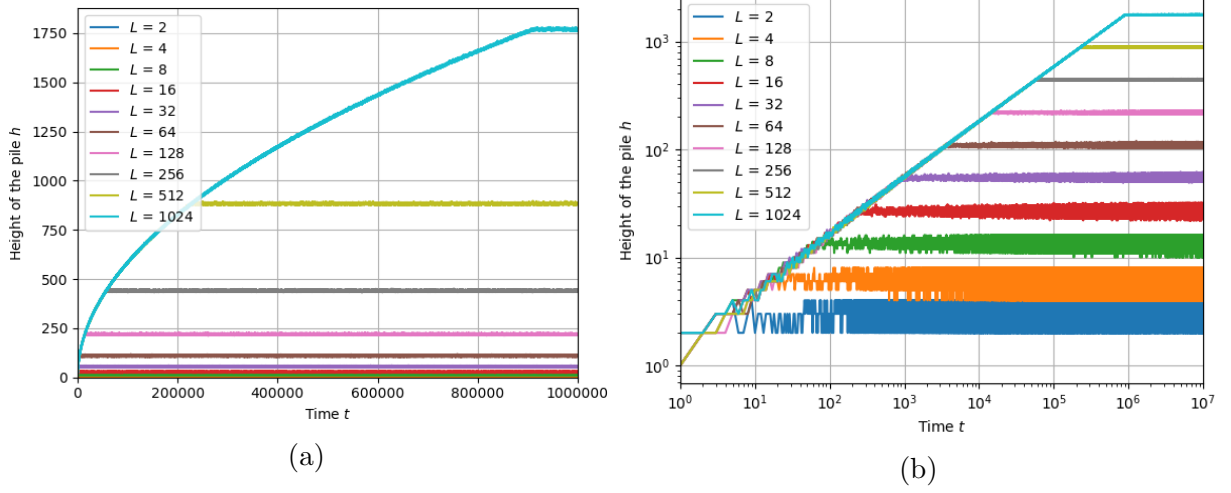
4

Figure 3: Graphs of height $h(t; L)$ against time t in (a) linear and (b) log-log scale. It can be seen that the height first increased with a power law, then fluctuated around a stable average.
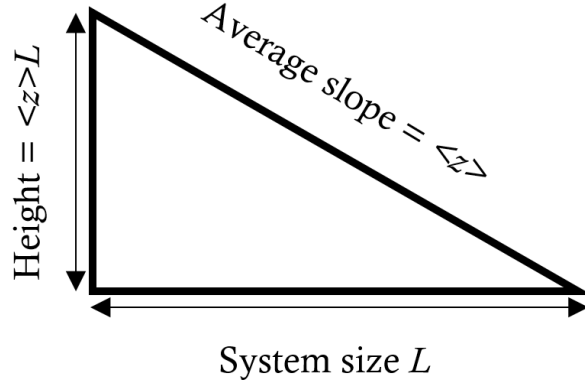

Figure 4: Diagram of the pile with a large L approximation of smoothed-out slopes like a triangle. The height can be approximated as $\langle z \rangle L$ and the cross-over time as $\langle z \rangle L^2 / 2$, the area of the triangle.

A data collapse can then be performed on Figure 3b by introducing the scaling relationship

$$\frac{\tilde{h}(t; L)}{L} = F\left(\frac{t}{L^2}\right), \tag{4}$$

where $\tilde{h}(t; L)$ is the smoothed height averaged over 25 neighbouring points, and $F\left(t/L^2\right)$ is the scaling function, to remove the dependence on L.

Figure 5 shows the result of the data collapse. It can be seen that $F(x)$ behaves as

$$F(x) \propto \begin{cases} x^{0.51134} & \text{for} \quad x \ll 1 \\ x^0 & \text{for} \quad x \gg 1. \end{cases} \tag{5}$$

5

as expected, since for large t (recurrent) the height was approximately constant, while for small t (transient), the time increased as the area of the triangle $\propto L^2$ and the height $\propto L$, so the height as a function of time should scale as $h \propto \sqrt{t} = t^{0.5}$. The slope of the linear fit 0.51134 ± 0.00004 was close to the expected value of 0.5.
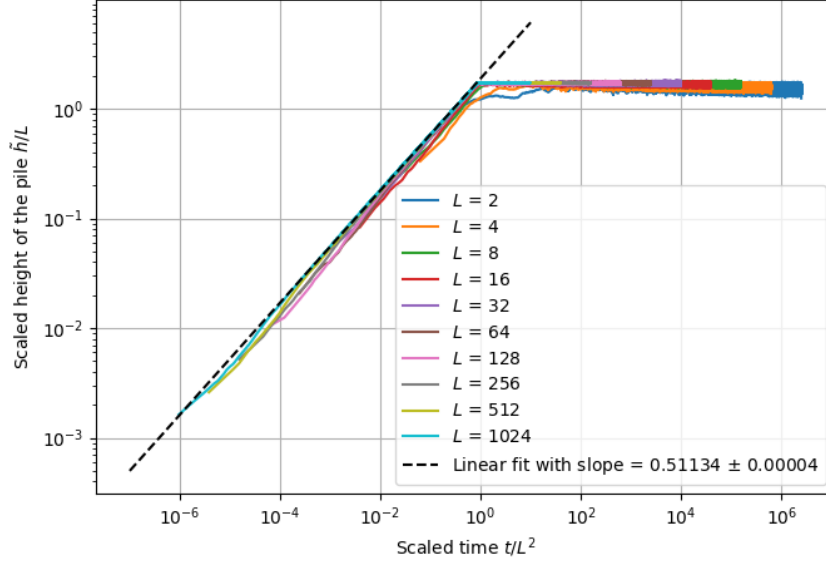

Figure 5: Graph showing the data collapse of scaled and smoothed height $\tilde{h}(t; L)/L$ against scaled time t/L^2. The slope of the linear fit (using `numpy.polyfit` with degree 1) along the transient was used to determine the behaviour of $F(t/L^2)$ for small t.

3.3 Corrections to scaling of average cross-over time $\langle t_c(L) \rangle$ - Task 2d

The cross-over time can be expressed in terms of the sum of local slopes when an added grain induced a grain to leave the system z_i at all sites i as

$$t_c(L) = \sum_{i=1}^{L} z_i \cdot i. \tag{6}$$

Averaging this gives

$$
\begin{aligned}
\langle t_c(L) \rangle &= \langle z_i \rangle \sum_{i=1}^{L} i \\
&= \frac{(1+L)L}{2} \langle z_i \rangle \\
&= \frac{\langle z \rangle}{2} L^2 \left(1 + \frac{1}{L}\right),
\end{aligned} \tag{7}
$$

assuming the average of all local slopes is equal to the true average slope, i.e. $\langle z_i \rangle = \langle z \rangle$. The $1/L$ term is the correction to scaling and is significant when L is small.

Equation 7 was examined using simulated cross-over times averaged over 2×10^4 values for sizes $L = 4, 8, 16, 32, 64, 128, 256$.

3.3.1 $\langle t_c(L) \rangle \propto L^2$

Taking the logarithm of equation 7 gives

$$\log\langle t_c(L) \rangle = 2\log L + \log\left[\frac{\langle z \rangle}{2}\left(1 + \frac{1}{L}\right)\right], \tag{8}$$

meaning that a log-log fitting of $\langle t_c(L) \rangle$ against L should yield a slope of 2. Figure 6 shows the log-log plot with a linear fitting. The slope of the fitted line is 1.978 ± 0.016, which was consistent with the theoretical prediction.
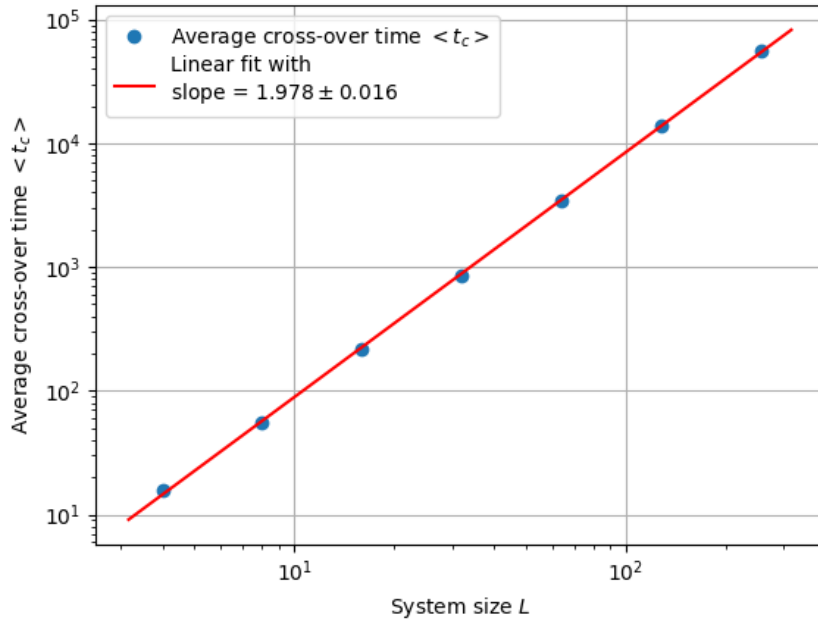

Figure 6: Log-log plot and linear fit of average cross-over time $\langle t_c(L) \rangle$ against system size L. The slope of the fitted line is 1.978 ± 0.016, consistent with the theoretical prediction of 2.

3.3.2 $\langle t_c(L) \rangle \propto \langle z \rangle$ and $\langle t_c(L) \rangle \propto (1 + 1/L)$ at different L

From equation 7, it is expected that on a plot of $\langle t_c(L) \rangle / L^2 = \langle z \rangle (1 + 1/L)/2$ against L, there is an asymptotic behaviour towards $\langle z \rangle / 2$ as $L \to \infty$. The experimental plot is shown in Figure 7. When $L \to \infty$, both theoretical and experimental values tend towards the constant value of 0.86, showing that correction to scaling is only significant for small L, and can be neglected when L is large. The general trend of the theoretical relation was confirmed by experimental data, but the values are all lower than expected. This may be due to an overestimate of the average slope $\langle z_i \rangle$ above $\langle z \rangle$ in the theoretical relation as the simulated system had an average slope that tends to 2.
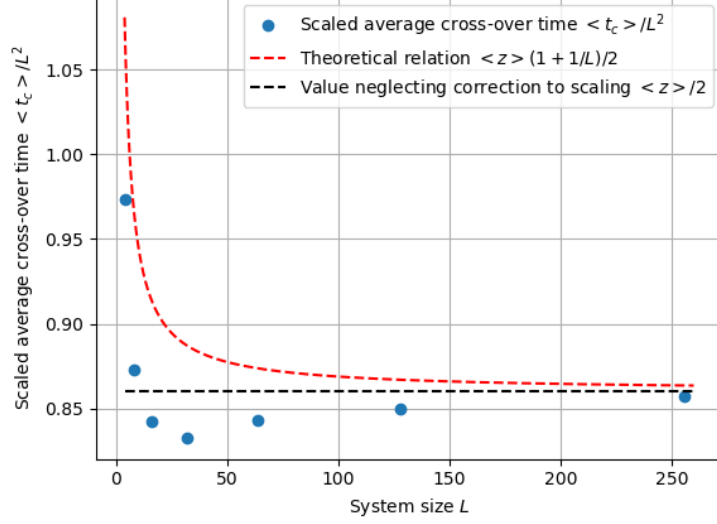
7

Figure 7: Graph of $\langle t_c(L)\rangle/L^2 = \langle z\rangle(1 + 1/L)/2$ against L, together with theoretical prediction of the correction to scaling, and the constant value if correction to scaling is neglected.

4 Average height $\langle h(t; L)\rangle$, standard deviation of height $\sigma_h(L)$ and height probability $P(h; L)$

4.1 Average height $\langle h(t; L)\rangle$ - Task 2e

The average height after recurrence is given by [4]

$$\langle h(t; L)\rangle_t = \lim_{T\to\infty} \frac{1}{T} \sum_{t=t_0+1}^{t_0+T} h(t; L), \tag{9}$$

where T is the number of points to average over and $t_0 > t_c(L)$ is a time after recurrence is reached. Here $t_0 = 2L^2$ to ensure steady state was reached and the number of heights averaged T ranged from around 8×10^6 to 9.9×10^6 for different system sizes L, close to 10^7 and can be approximated as infinity. Ignoring corrections to scaling, a linear fit was performed on a plot of average height $\langle h(t; L)\rangle$ against system size L and is shown in Figure 8.

The existence of a non-zero intercept showed that height was not exactly proportional to system size as described in section 3.2. A correction to scaling was introduced and assumed to take the form of

$$\langle h(t; L)\rangle_t = a_0 L(1 - a_1 L^{-\omega_1} + O(L^{-\omega_2})), \tag{10}$$

where a_i are constants and $\omega_i > 0$. Neglecting $O(L^{-\omega_2})$ terms and taking the logarithm of this relation gives

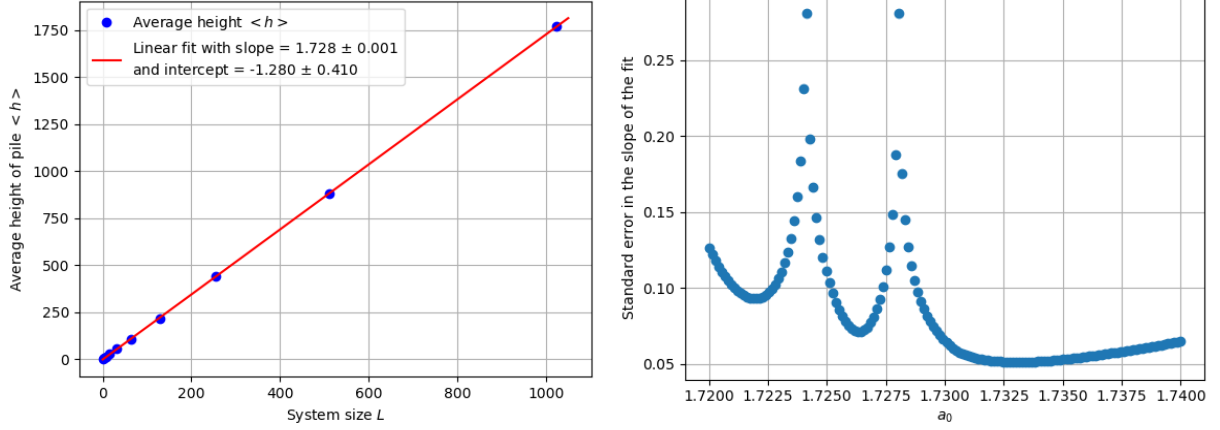$$\log\left(a_0 - \frac{\langle h(t; L)\rangle_t}{L}\right) = -\omega_1 \log L + \log a_0 + \log a_1, \tag{11}$$

8

Figure 8: Graph of average height $\langle h(t; L)\rangle_t$ against system size L with a linear fit. The slope $a_0 = 1.728 \pm 0.001$ is the average slope of the pile and the non-zero intercept shows that correction to scaling is significant.

Figure 9: Graph of standard error in the slope of linear fitting on a log-log plot of $a_0 - \langle h(t; L)\rangle_t/L$ against L for a_0 ranging from 1.720 to 1.740. The minimum is found to be at $a_0 = 1.733 \pm 0.001$.

meaning that the slope of a linear fitting on a log-log plot of $a_0 - \langle h(t; L)\rangle_t/L$ against L should yield an accurate value of $-\omega_1$ if a_0 is chosen correctly.

Using the approximate value of $a_0 \approx 1.730$ in Figure 8 as a starting point, 150 values of a_0 in the range of 1.720 to 1.740 were tried in fitting equation 11, and the standard errors of the slope were computed and compared in Figure 9. The best fit was found with $a_0 = 1.733 \pm 0.001$. This was then used to produce a linear fitting of equation 11 as shown in Figure 10. From equation 11, the slope corresponds to $-\omega_1$ so $\omega_1 = 0.578 \pm 0.026$ and the intercept corresponds to $\log a_0 + \log a_1$ so $a_1 = 0.191 \pm 0.015$.

4.2 Standard deviation of height $\sigma_h(L)$ - Task 2f

The standard deviation after recurrence is given by [4]

$$
\begin{aligned}
\sigma_h(L) &= \sqrt{\langle h^2(t; L)\rangle_t - \langle h(t; L)\rangle_t^2} \\
&= \sqrt{\lim_{T\to\infty} \frac{1}{T} \sum_{t=t_0+1}^{t_0+T} h^2(t; L) - \left[\lim_{T\to\infty} \frac{1}{T} \sum_{t=t_0+1}^{t_0+T} h(t; L)\right]^2},
\end{aligned}
\tag{12}
$$

where $T \approx 10^7$ and $t_0 = 2L^2$ again. Since the standard deviation has no known relationship with system size L, a more general form of the scaling relationship than in equation 10 is proposed as

$$
\sigma_h(L) = a_0 L^{\omega_0}(1 - a_1 L^{-\omega_1} + O(L^{-\omega_2})),
\tag{13}
$$

introducing ω_0 as the unknown exponent on the scaling L. Using `scipy.optimize.curve_fit`, this function was fitted to a plot of experimental $\sigma_h(L)$ against system size L, as shown in Figure 11. The parameters were determined to be $a_0 = 0.079 \pm 0.005$, $\omega_0 = 0.239 \pm 0.068$, $a_1 = 0.929 \pm 0.051$ and $\omega_1 = 3.559 \pm 0.130$. From Figure 11b, as L becomes large, the
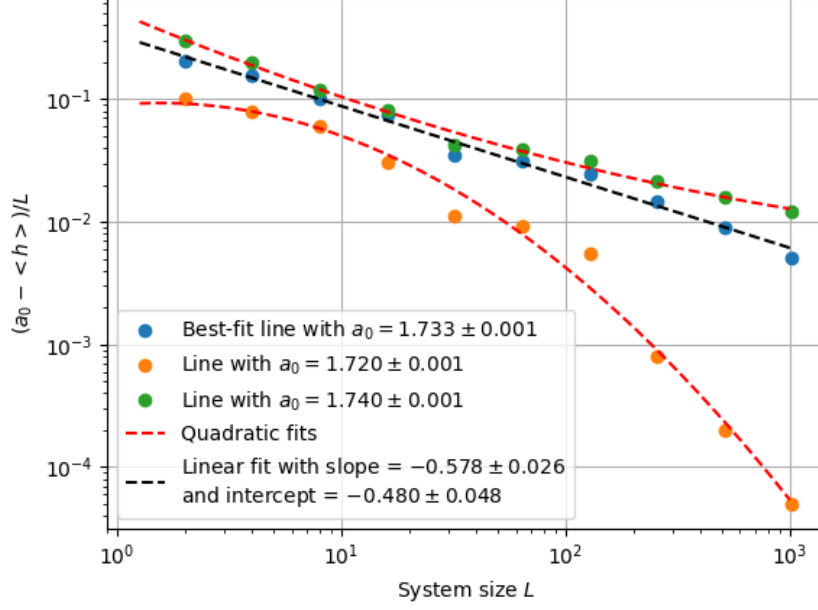
9

Figure 10: Graph of $a_0 - \langle h(t; L) \rangle_t / L$ against L, for the best fit $a_0 = 1.733 \pm 0.001$ and $a_0 = 1.720 \pm 0.001$ and $a_0 = 1.740 \pm 0.001$ for comparison. A linear fit was performed for $a_0 = 1.733$, and the slope and intercept were then used to obtain ω_1 and a_1 respectively. Quadratic fits were performed on the other two to show the deviation from linearity due to inaccuracy in a_0.

standard deviation tends towards $a_0 L^{\omega_0}$. For smaller L, $\sigma_h(L)$ decreases as the correction to scaling $a_1 L^{-\omega_1}$ is significant.
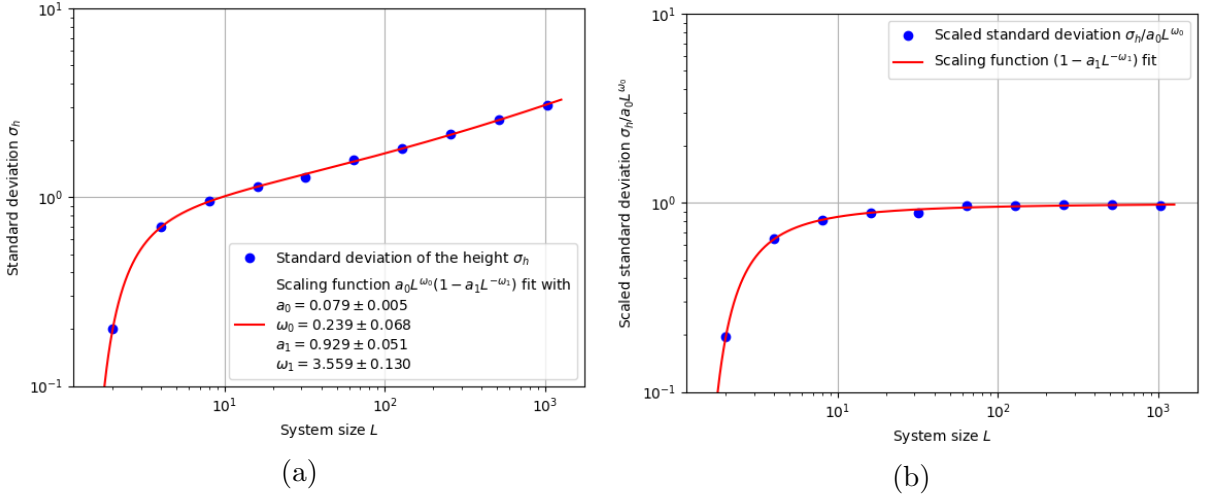

(a)

(b)

Figure 11: Graphs of standard deviation $\sigma_h(L)$ against system size L, both (a) unscaled and (b) scaled with $a_0 L^{\omega_0}$. The corrections to scaling functions fitted are (a) $a_0 L^{\omega_0}(1 - a_1 L^{-\omega_1})$ and (b) $1 - a_1 L^{-\omega_1}$.

The height of the pile can be defined as the sum of local slopes across all sites i at

time t, i.e.

$$h(t; L) = \sum_{i=1}^{L} z_i(t), \tag{14}$$

as $z_i = h_i - h_{i+1}$ and $h_{L+1} = 0$. Comparing with the expression for the average slope $z(t; L)$ over all *sites i* at a time t,

$$z(t; L) = \frac{1}{L} \sum_{i=1}^{L} z_i(t) = \frac{1}{L} h(t; L), \tag{15}$$

means that the scaling relations of average height and standard deviation of height, equations 10 and 13, can be directly applied to the average slope $\langle z \rangle_t$ over all *times t* after recurrence and its standard deviation by

$$\langle z \rangle_t = \frac{1}{L} \langle h \rangle_t = a_{0h}(1 - a_{1h} L^{-\omega_{1h}}), \tag{16}$$

$$\langle z^2 \rangle_t = \frac{1}{L} \langle h^2 \rangle_t, \tag{17}$$

and so

$$\sigma_z = \sqrt{\langle z^2 \rangle_t - \langle z \rangle_t^2} = \frac{1}{L} \sqrt{\langle h^2 \rangle_t - \langle h \rangle_t^2} = \frac{1}{L} \sigma_h$$
$$= a_{0\sigma} L^{\omega_{0\sigma}-1}(1 - a_{1\sigma} L^{-\omega_{1\sigma}}), \tag{18}$$

where subscripts h and σ denote the parameters of the respective scaling function. In the limit $L \to \infty$, the correction terms are expected to vanish and so $\langle z \rangle_t \to a_{0h}$ and $\sigma_z \to a_{0\sigma} L^{\omega_{0\sigma}-1} \to 0$ as $\omega_{0\sigma} = 0.239 < 1$ so the exponent is negative.

4.3 Probability of height after recurrence $P(h; L)$ - Task 2g

The height probability $P(h; L)$ is defined as [4] the ratio between the number of observed configurations with height h in a pile of size L and the total number of observed configurations. Using the definition of height in equation 14, and assuming that z_i are independent and identically distributed random variables with finite variance, by the Central Limit Theorem, the height is also a random variable and its probability distribution is expected to follow a Gaussian distribution when $L \gg 1$.

The height probability $P(h; L)$ was measured as shown in Figure 12. The shapes of each curve are approximately Gaussian. Using the expression for a Gaussian distribution and substituting the scaling relations for $\langle h \rangle_t$ and σ_h,

$$P(h; L) = \frac{1}{\sigma_h \sqrt{2\pi}} \exp\left(-\frac{(h - \langle h \rangle_t)^2}{2\sigma_h^2}\right)$$
$$= \frac{1}{a_{0\sigma} L^{\omega_{0\sigma}} \sqrt{2\pi}} \exp\left(-\frac{(h - a_{0h} L(1 - a_{1h} L^{-\omega_{1h}}))^2}{2a_{0\sigma}^2 L^{2\omega_{0\sigma}}}\right). \tag{19}$$

Taking logarithm and rearranging,

$$\ln\left(a_{0\sigma} L^{\omega_{0\sigma}} \sqrt{2\pi} P(h; L)\right) = -\frac{(h - a_{0h} L(1 - a_{1h} L^{-\omega_{1h}}))^2}{2a_{0\sigma}^2 L^{2\omega_{0\sigma}}}. \tag{20}$$

11

So, by scaling the height $h' = (h - a_{0h}L(1 - a_{1h}L^{-\omega_{1h}}))/L^{\omega_{0\sigma}}$ and the probability $P' = a_{0\sigma}L^{\omega_{0\sigma}}\sqrt{2\pi}P(h; L) \propto L^{\omega_{0\sigma}}P(h; L)$, a data collapse can be performed on Figure 12. The collapsed data was then fitted with a Gaussian curve as shown in Figure 13a with a mean of $\langle h' \rangle$. The mean of the scaled height $\langle h' \rangle$ is expected to be zero as the scaled height is just the deviation from the average height.
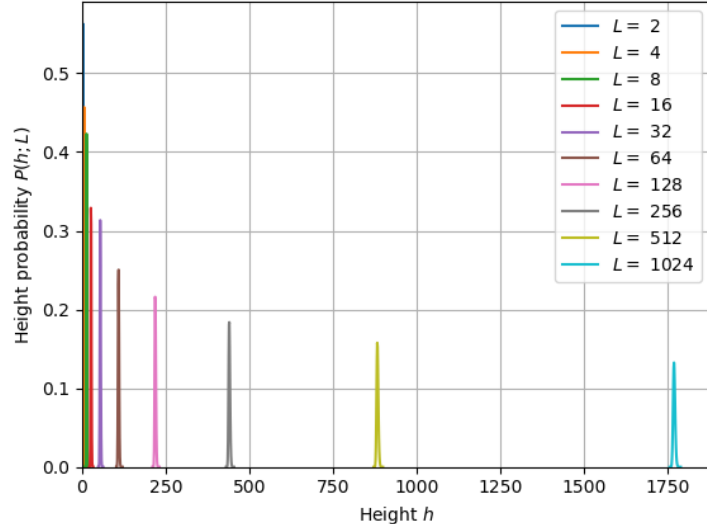

Figure 12: Graph of height probability $P(h; L)$ against height h for a range of system size L. It can be seen that the shapes of each curve are approximately Gaussian with an increasing width but decreasing height as L increases.

There is an asymmetry in Figure 13a, where there are more data greater than the average height and to a higher maximum (40 as opposed to -30). This is clearly seen when a linear-x log-y scale was used instead to plot the same diagram using equation 20, as shown in Figure 13b. This can be explained using the fact that local slopes of 2 tend to be favoured as fewer avalanches are triggered when a grain is added. So, the system tends to a height greater than average more often.

5   Avalanche-size probability $P(s; L)$

The size of an avalanche s is the number of relaxations triggered by the addition of a grain. The avalanche-size probability $P_N(s; L)$ is defined as the ratio between the number of avalanches of size s in a system of size L and the total number of avalanche N.

5.1   Log-binning and poor statistics

Log-binning is a useful method to extract information on probability which is present in a noisy tail where statistics are poor [2], by exponentially increasing the size of each bin in the histogram using a scale factor $a > 1$, so the j-th bin covers the interval $[a^j, a^{j+1}]$ and more points can be covered in a bin where data points are spread out. A number of a values were tested. If a is too small, some of the bins may not contain a data point, so
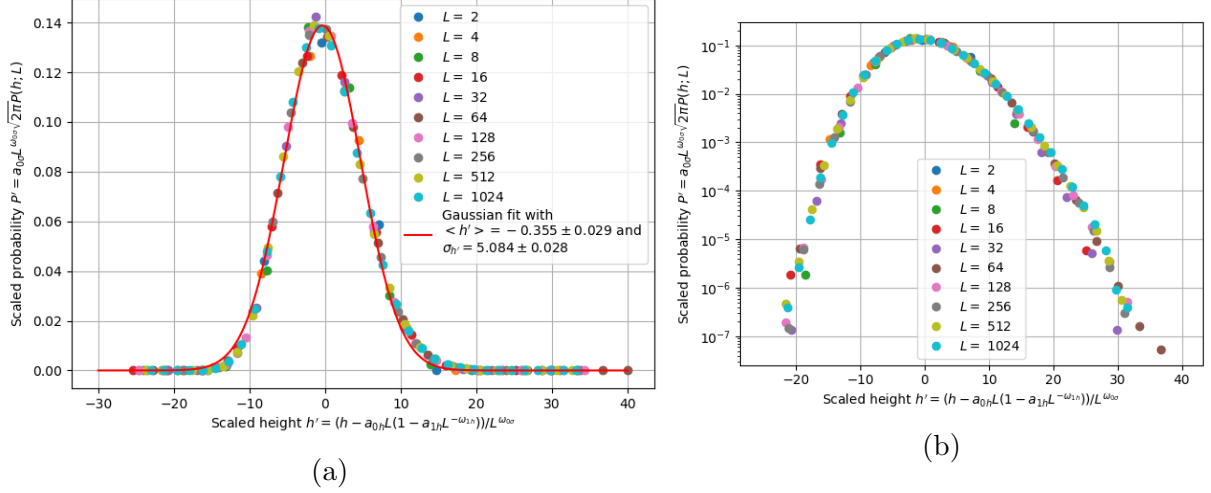
Figure 13: Graphs showing the data collapse of the scaled height probability $P' = a_{0\sigma}L^{\omega_{0\sigma}}\sqrt{2\pi}P(h;L)$ against the scaled height $h' = (h - a_{0h}L(1 - a_{1h}L^{-\omega_{1h}}))/L^{\omega_{0\sigma}}$ on (a) linear and (b) log-y scales. It can be clearly seen that the probability of having a height of larger than the average is greater than otherwise.

empty bins will produce discontinuities in the curve. If a is too large, the log-binning is less effective in smoothing out the data as the difference in the current bin centre and the next is too large. The optimal value found for this analysis is $a = 1.5$.

The true underlying avalanche-size probability $P(s)$ is defined as

$$P(s) = \lim_{N\to\infty} P_N(s) \approx P_N(s) \quad \text{for} \quad N \gg 1. \tag{21}$$

In order to reveal $P(s)$, N needs to be sufficiently large enough. A number of N have been tried, ranging from 10^4 to 8×10^6, as shown in Figure 14 for $L = 1024$. When N is small, there are insufficient statistics to reveal the cutoff of $P(s)$, as can be seen in the $N = 10^4, 10^5$ cases. It is determined that there needs to be at least 10^6 points to capture the cutoff avalanche size.

5.2 Avalanche-size probability cutoff - Task 3a

In light of this, all the avalanche sizes after $t_0 = 2L^2$ were measured (around 8 to 9.9 $\times 10^6$ points), and the resultant log-binned probability $\tilde{P}(s;L)$ was plotted against system size L as shown in Figure 15. The log-binning also included avalanches of size 0 for normalisation purposes. It can be seen that the probability for a given avalanche size is the same for all L (as the linear part stacks up). Moreover, the probability decays as a power law of the avalanche size, however, there is a cutoff avalanche size for each L above which the avalanche-size probability drops rapidly and this increases with L. This can be explained due to the fact that the avalanche size is limited to a finite maximum due to the finite system size L, and the maximum increases with L.
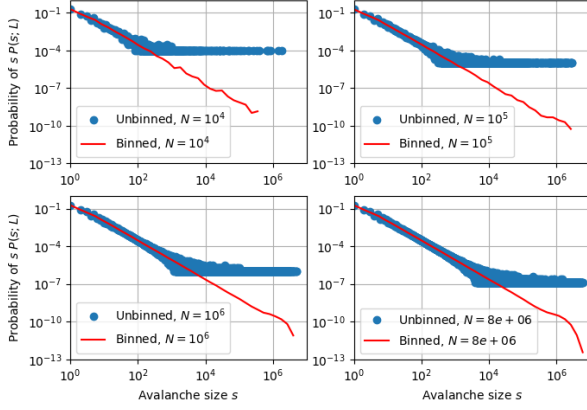
13

Figure 14: Graphs of unbinned $P(s; L)$ and log-binned avalanche-size probability $\tilde{P}(s; L)$ against avalanche size s for number of data points $N = 10^4, 10^5, 10^6, 8 \times 10^6$ (maximum amount of points after recurrence), for $L = 1024$.
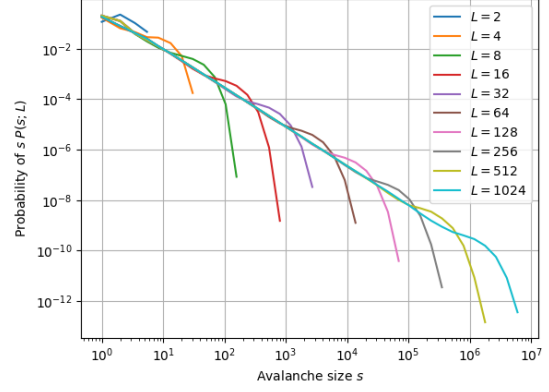

Figure 15: Graph of log-binned avalanche-size probability $\tilde{P}(s; L)$ against avalanche size s with scale factor $a = 1.5$. There is a cutoff avalanche size for each L above which the avalanche-size probability drops rapidly.

5.3 Finite-size scaling ansatz - Task 3b

The finite-size scaling ansatz for the avalanche-size probability is proposed as [4]

$$\tilde{P}_N(s; L) \propto s^{-\tau_s} \mathcal{G}(s/s_c),$$
$$s_c(L) \propto L^D, \tag{22}$$

for $L \gg 1, s \gg 1$, where s_c is the cutoff avalanche size, τ_s is the avalanche-size exponent and D is the avalanche dimension. Rearranging gives

$$\tilde{P}_N(s; L) \propto s^{-\tau_s} \mathcal{G}(s/L^D)$$
$$\log\left(\tilde{P}_N(s; L)\right) \propto -\tau_s \log s + \log\left(\mathcal{G}(s/L^D)\right). \tag{23}$$

When $L \gg 1$, the scaling function $\mathcal{G}$ tends to a constant as $s/L^D \to 0$. This means that the linear part of the log-log plot of $\tilde{P}_N(s; L)$ against s as in Figure 15 (between 10^2 and 10^4) should yield a slope of $-\tau_s$. Defining s_c as the point on the 'bump' with the maximum difference from the linear trend, fitting a log-log plot of s_c against L should yield a slope of D from equation 22. Using experimental values, τ_s and D were determined to be 1.553 ± 0.002 and 2.074 ± 0.034 respectively.

Using these values and the ansatz (equation 23), data collapse was performed on Figure 15, as shown in Figure 16.

For the boundary-driven Oslo model, the relationship between D and τ_s can be obtained as [2] (see Section 5.4 for derivation)

$$D(2 - \tau_s) = 1. \tag{24}$$

Using experimental values, $D(2-\tau_s) = 0.927 \pm 0.034$, close to the theoretical value. There was a larger uncertainty in obtaining D, due to the large uncertainty in estimating s_c.
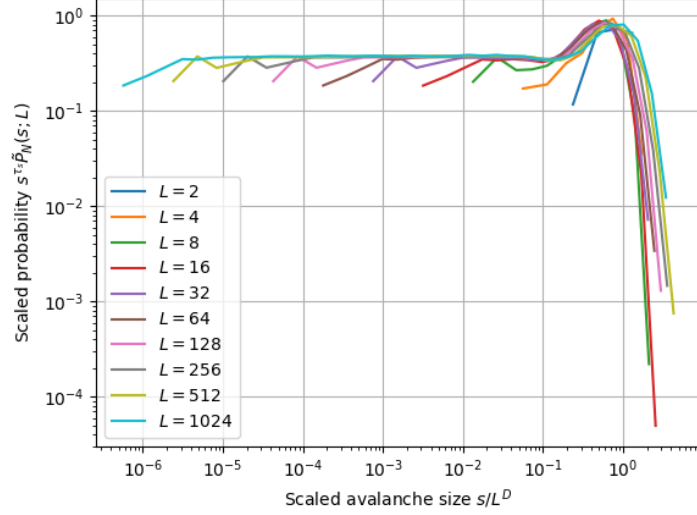
14

Figure 16: Graph showing the data collapse of scaled log-binned avalanche-size probability $s^{\tau_s}\tilde{P}_N(s;L)$ against scaled avalanche size s/L^D using $\tau_s = 1.553 \pm 0.002$ and $D = 2.074 \pm 0.034$.

5.4 Moment analysis - measurement of k'th moment of avalanche size $\langle s^k \rangle$ - Task 3c

The k'th moment of avalanche size $\langle s^k \rangle$ can be measured by

$$\langle s^k \rangle = \lim_{T \to \infty} \frac{1}{T} \sum_{t=t_0+1}^{t_0+T} s_t^k, \tag{25}$$

where s_t is the measured avalanche size at time t and $t_0 = 2L^2$ again. Avalanches of size 0 were included in the analysis again. The experimental k'th moment was calculated and plotted in Figure 17. Clearly, the k'th moment scales with a power law of L.

The k'th moment is properly defined as [2]

$$
\begin{aligned}
\langle s^k \rangle &= \sum_{s=1}^{\infty} s^k P(s;L) \\
&= \sum_{s=1}^{\infty} s^{k-\tau_s} \mathcal{G}(s/L^D) \quad \text{using the ansatz (equation 22)} \\
&\propto \int_1^{\infty} s^{k-\tau_s} \mathcal{G}(s/L^D) ds \\
&= \int_{1/L^D}^{\infty} (uL^D)^{k-\tau_s} \mathcal{G}(u) L^D du \quad \text{where} \quad u = s/L^D \\
&= L^{D(1+k-\tau_s)} \int_{1/L^D}^{\infty} u^{k-\tau_s} \mathcal{G}(u) du.
\end{aligned}
\tag{26}
$$

When $L \gg 1$, the lower limit of the integral tends to zero, and so the integral tends to a constant as long as $1 + k - \tau_s > 0$ in the lower limit. In the upper limit, $\mathcal{G}(u)$ decays
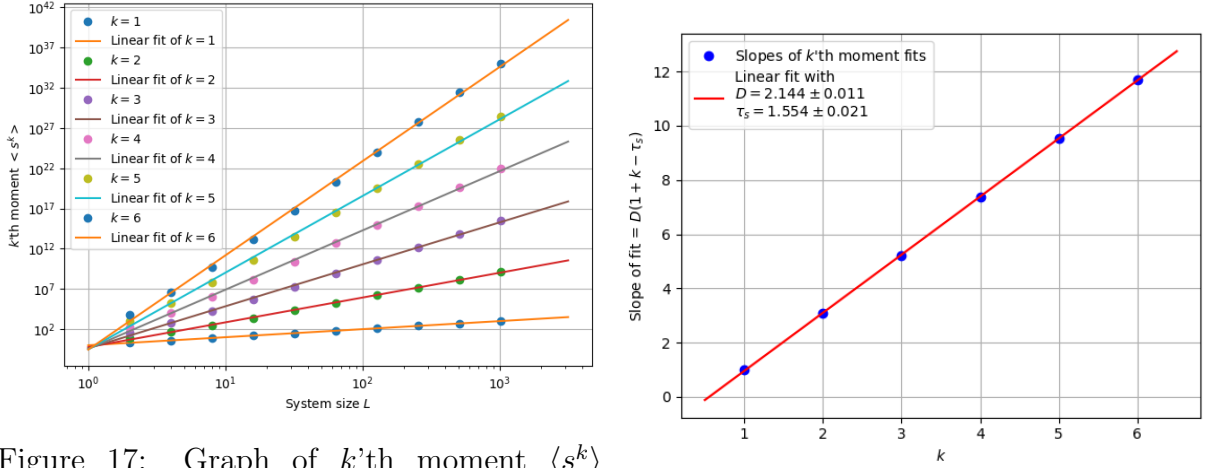
15

Figure 17: Graph of k'th moment $\langle s^k \rangle$ against system size L, for $k = 1, 2, 3, 4, 5, 6$. There is a linear trend for all 6 moments, meaning that they scale with a power of L.

Figure 18: Linear fit of slope of each moment $m = Dk + D(1 - \tau_s)$ against k.

sufficiently rapidly to ensure convergence. So the k'th moment

$$
\begin{aligned}
\langle s^k \rangle &\propto L^{D(1+k-\tau_s)}, \quad \text{or} \\
\log\langle s^k \rangle &\propto D(1 + k - \tau_s) \log L,
\end{aligned}
\tag{27}
$$

for $L \gg 1, k \geq 1$.

To extract D and τ_s, the slope of each moment $m = Dk + D(1 - \tau_s)$ was plotted against k, and the slope and intercept were used to find D and τ_s respectively. This is as shown in Figure 18. From this method, D and τ_s was found to be 2.144 ± 0.011 and 1.554 ± 0.021 respectively.

After recurrence, on average, one added grain should induce one grain to leave the system, so the average avalanche size $\langle s \rangle \propto L$. Inserting $k = 1$ for Oslo model into equation 27 gives also $\langle s \rangle \propto L^{D(2-\tau_s)}$. Equating the two exponent yields equation 24. Using the experimental values, $D(2 - \tau_s) = 0.956 \pm 0.124$, confirming with theoretical prediction.

A closer look at Figure 17 shows that the linear fits do not cross at the origin, indicating a sign of correction to scaling. Assuming the form of correction to scaling form as in equation 13, $a_0 L^{\omega_0}(1 - a_1 L^{-\omega_1})$, this was applied to the 6 moments following a similar approach as in Section 4.2. The scaled moments were then plotted against system size L similar to Figure 11b, as shown in Figure 19. It is notable that the first moment is not subject to corrections to scaling as $a_1 = 0$, but all higher moments require a correction term, and these increase in magnitude, most likely because the corrections are amplified with higher powers of s.

6   Conclusion

The Oslo model was implemented and studied, with particular respect to the height and avalanche size of the pile. Scaling relationships and their parameters were determined
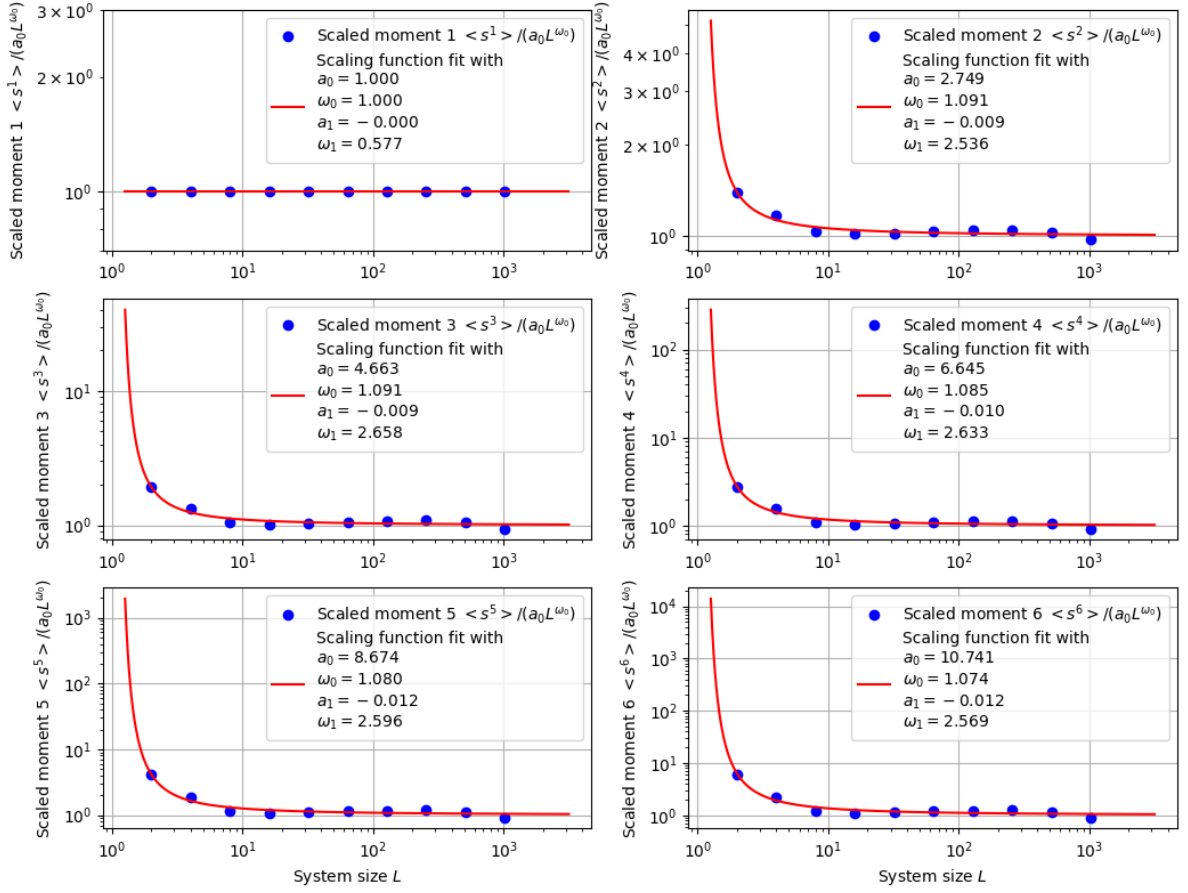
16

Figure 19: Graph of scaled k'th moments against system size L, with scaling functions fitted $1 - a_1 L^{-\omega_1}$, for $k =$ 1, 2, 3, 4, 5, 6.

for the height, height probability and avalanche size probability, followed by data collapse to reveal the scale-free behaviour of such a system. These were found to follow a power law and had a finite cutoff because the system size was finite. Corrections to scaling were found to be significant with small system sizes for the cross-over time, average height and its standard deviation, and also the second and above moments of avalanche-size probability.

References

[1] Bak P, Tang C, Wiesenfeld K. *Self-Organized Criticality: An Explanation of 1/f Noise.* Physical Review Letters. 1987 Mar;59(381):381–384.

[2] Christensen K, Moloney NR. *Complexity and Criticality.* Imperial College Press; 2005.

[3] Christensen K, Corral A, Frette V, Feder J, Jøssang T. *Tracer Dispersion in a Self-Organized Critical System.* Physical Review Letters. 1996 Jan;77(1):107–110.

[4] Christensen K. *Complexity Project Notes.* Imperial College London; 2018.